МОДЕЛЮВАННЯ ОПЕРАЦІЙ ТА БОЙОВИХ ДІЙ У ПОВІТРЯНОМУ ПРОСТОРІ

DOI 10.33099/2786-7714-2026-1-10-72-81

УДК 621.396.96

Dmytro Zavadsky
https://orcid.org/0000-0003-2728-136X
Oleh Biloborodov (Doctor of Technical Sciences, Senior Researcher)
https://orcid.org/0000-0003-3166-2659

Central Research Institute of Armament and Military Equipment of the Armed Forces of Ukraine, Kyiv, Ukraine

Received: November 21, 2025; Accepted: May 16, 2026; Published: June 17, 2026.

RESEARCH ON THE CHARACTERISTICS OF RADAR DETECTABILITY OF RUSSIAN AIR ATTACK WEAPONS USING 3D MODELLING TECHNOLOGIES

The article presents scientific and methodological approaches and research results on the characteristics of radar visibility of modern enemy air attack weapons using numerical modelling methods. To conduct the software experiment, a software and hardware complex for modelling high-frequency aspects of the functioning of weapons and military equipment samples based on Ansys Academic Research HF is used in combination with parametric 3D modelling in SolidWorks and similar CAD systems. 3D models of the main Russian air attack weapons have been created and studied. Particular attention was paid to determining the electromagnetic properties of materials used in the designs of the samples using the NIST methodology, with the parameters obtained subsequently entered into the modelling environment. A series of software experiments was conducted across a wide frequency range to assess the effective scattering area for different irradiation angles. The results obtained made it possible to determine the statistical characteristics of the radar visibility of various types of air targets, to identify the influence of geometry and materials on the effective scattering area, and to provide a basis for further research in the field of radar detection and tracking of airborne objects.

Keywords: *radar visibility, effective scattering area, air attack weapons, 3D modelling, Ansys HFSS, electromagnetic properties of materials.*

INTRODUCTION

The experience of armed conflict has shown that the enemy is well equipped with various types of air attack weapons (AAW): strike FPV drones and drones with drop-offs, bomb weapons with aerodynamic gliding equipment, long-range strike UAVs, ground-, air- and sea-launched cruise missiles, ground-launched ballistic missiles, and air-launched aeroballistic missiles. Assessment of the current air situation is based on information obtained by deployed sensor systems: optical, acoustic, radio technical reconnaissance, and radar surveillance. Radar systems have the greatest information capabilities, differing in both range and a wide range of observation conditions [1].

To reduce situational awareness of the air situation, the enemy uses a number of technical and tactical measures: the use of radar-invisible shapes, anti-radar coatings, passive (dipole) jammers, and false air targets in modern models, and when choosing routes, the features of the terrain and gaps in the radar field are often used. A comprehensive study of air threat detection at the present stage requires research into the radar visibility characteristics of UAVs and further improvement of models for detecting and tracking airborne objects, taking into account the observation angle and terrain conditions, which determines the relevance of the study. The main characteristic of radar visibility is the effective scattering area. Its value is determined by the electrical and magnetic properties of the object's material, its spatial configuration, the ratio of its dimensions to the wavelength of radiation, and the orientation of the object relative to the direction of radiation. Existing methods of high-frequency analysis allow obtaining sufficiently accurate analytical solutions for calculating the effective scattering area of objects of simple geometric shape [2, 4]. Real objects of practical interest consist of a large number of details of various shapes, orientations and materials. A large number of recent studies have been aimed at improving calculation methods by simplifying radar cross section RCS models through recalculating the radar visibility characteristics of simple geometric shapes [4, 5]. At the same time, researchers note a significant (by orders of magnitude) change in the RCS of UAVs when the observation angle changes [2, 7]. Many studies are devoted to analyzing the radar visibility characteristics of the most common airborne objects [3, 8-17].

The following indicators are used to assess radar visibility [1,5, 6, 17-18]:

directly the graph of the dependence of the RCS

value on the angular coordinates of the irradiation;

numerical indicators of characteristic sections of the specified graph (local and global maximum/minimum values and corresponding angular indicators);

statistical characteristics (mean value, median, statistics of width, asymmetry and kurtosis);

statistical characteristics in angular sectors from 5 to 15 degrees in the azimuthal plane of object irradiation.

Materials and Methods

A wide range of studies is devoted to testing hypotheses about the distribution law (DL) of experimentally determined values of RCS (as well as the square root of RCS) from the composition of the inverse secondary radiation diagram for various objects. The null hypothesis uses normal PD [5, 7], Rayleigh [5, 6, 19], lognormal [5, 19], $\chi 2$ type [6], Weibull [5], Guerra-Tippett [19] and others.

Scientific publications by specialized research institutions [19, 20] are devoted to the study of the radar visibility characteristics of air attack weapons. At the same time, experience in researching debris and captured samples of airborne attack vehicles requires in-depth study of design features, electromagnetic characteristics of materials, and other aspects of radar detection of real airborne objects.

The aim of the study was to summarize the practical experience gained and scientific and methodological approaches to studying the radar visibility characteristics of Russian air attack weapons.

Results

During the scientific and technical examination of the wreckage of the AAW using 3D scanning tools (Artec LEO), as well as by direct measurement, the dimensions, shape and design of the objects were determined, then determs the electromagnetic properties of materials, after which a software experiment was organized.

An important task in the creation of 3D models is the selection of an appropriate software editor. Modelling programs can be divided into several main types depending on their purpose and scope of application. The first type of programs (Blender, 3DS Max, Mayan, etc.) are 3D editors that use polygonal modelling and are designed to create three-dimensional models used in animation, visualisation, and other creative industries. In theory, this type of software can be used to perform the tasks at hand, but practical experience has shown that the further conversion of the model file into a suitable format is a problematic issue. The processes of exporting and importing files of different formats for complex models almost always lead to geometry errors, which in turn makes it impossible to obtain adequate calculation results. The second type of software (SolidWorks, NX, Compass-3D, Inventor, Fusion 360) uses parametric solid modelling, which creates models based on volumes, allowing you to accurately calculate and change the dimensions and shape of objects. It is this modelling method that is used to create AAW models (Fig. 1).

Further improvement of models. The next stage was the development of 3D models of AAW components, such as the ARGS-59E active radar homing head of the Kh-59MK missile, the Kh-101 navigation and guidance module (Fig. 2), etc. Thanks to the created 3D models of these components, the characteristics of radar visibility are refined and the reliability of the obtained model estimates is increased. The results obtained are planned to be used in the future to study the spatial location of directional diagrams during movement and to assess the capabilities of electronic warfare. At this stage, the electromagnetic properties of materials become an important factor, so the models are becoming increasingly complex: radio-absorbing coatings, radio-transparent domes and other elements are being added (Fig. 2e).

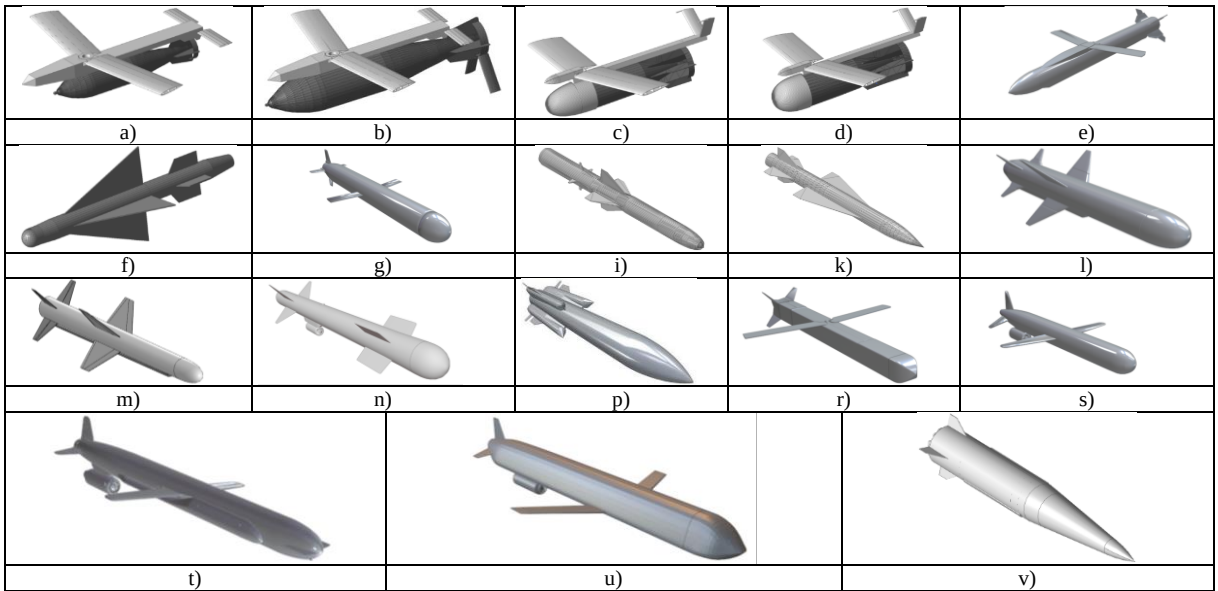

Figure 1. Solid-state 3D models of Russian airborne rocket and bomb weapons: a) FAB-250, equipped with UMPC (type 1) ; b) FAB-500 M62, equipped with UMPC (type 1); c) FAB-1500 M54, equipped with UMPC (type 2); d) FAB-3000, equipped with UMPC (type 2); e) Grom-1E; f) UPAB-1500V; g) 3M-14 Kalibr; i)

3M55 Onyx; k) Kh-22; l) Kh-35; m) Kh-38; n) Kh-59M2; p) Kh-31; r) Kh-69; s) Kh-55; t) Kh-555; u) Kh-101; f) 9-S-7760

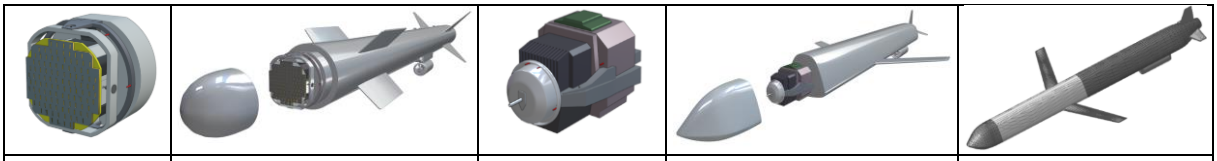

a) b) c) d) e)

Figure 2. Improvements to AAW models: a) ARGS-59E radar homing head from the Kh-59M2 missile; b) improved model of the Kh-59M2 missile with a radio-transparent dome and homing head; c) navigation and guidance module from the Kh-101 missile; d) improvement of the warhead of the Kh-101 missile model e) improvement of the Kh-101 missile model with the addition of dielectric (including radio-absorbing) materials

Models of unmanned aerial vehicles. In addition to the AAWs discussed above, the enemy is making massive use of Shahed-type strike UAVs across virtually the entire territory of Ukraine (Fig. 3).

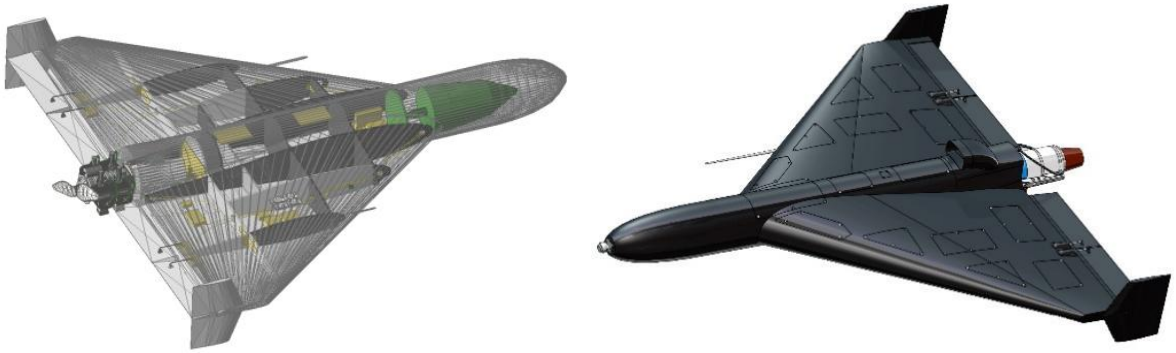

a) b)

Figure 3. 3D models of long-range unmanned strike vehicles:
a) Shahed-136 (Geran-2); b) Geran-3 (with a jet engine)

On the line of combat engagement and in tactical depth, the enemy uses copter-type UAVs (DJI, AUTEL), the most dangerous of which are strike FPV drones and drones with drop-offs (Fig. 4).

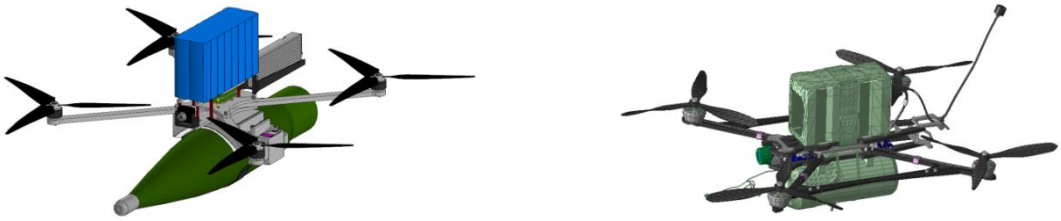

a) b)

Figure 4. 3D models of FPV drones: a) 10" FPV drone with a payload; b) 7" reconnaissance FPV drone

Research into aircraft-type unmanned aerial vehicles (such as ZALA, Orlan, Supercam, Merlin, Eleron, etc.) is limited by the extensive use of dielectric materials in their construction, which requires both additional materials research and significant computing resources for software modelling.

Determination of the electromagnetic properties of materials. The electromagnetic properties of individual materials from the AAW composition were determined in accordance with the methodology of the US National Institute of Standards and Technology [21, 22] in collaboration with Kyiv Academic University: material samples were divided into sections measuring approximately 1.5×4 cm and approximately 1.5 mm thick. The sections were then placed between the open ends of the waveguides, shielded with metal spacers and fixed by compression. After calibration at the surface level of the open flanges of the Thru-Reflect-Line (TRL) waveguide using the method [23], the S-parameters (i.e., transmission and reflection coefficients in the forward and reverse directions) were measured and converted into electromagnetic characteristics: dielectric permeability, dielectric loss tangent, magnetic permeability, magnetic loss tangent. The obtained electromagnetic characteristics of the materials were entered into the material properties in the modelling software package.

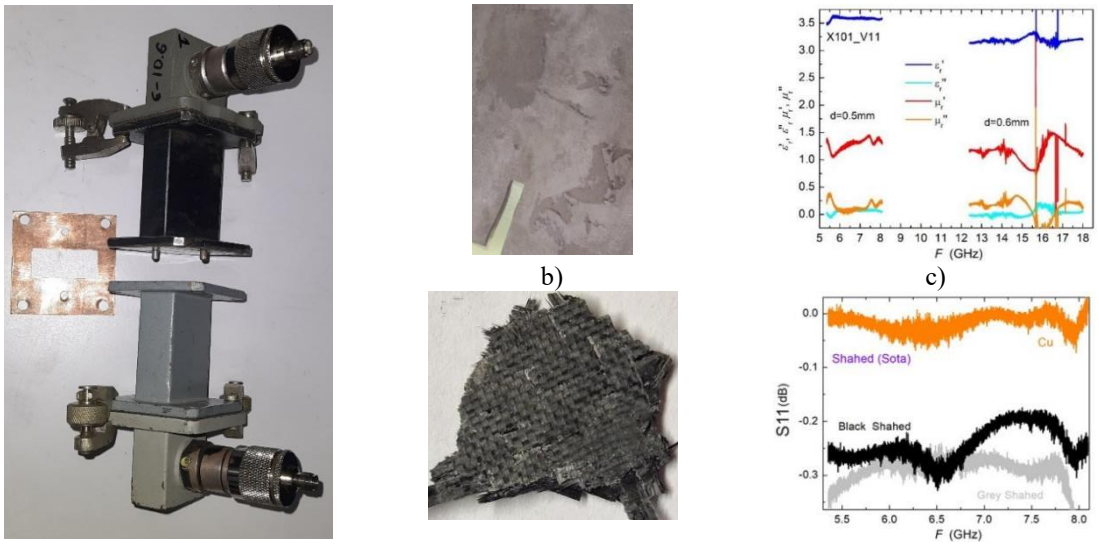

a) b) c) d) e)

Figure 5. Investigation of the electromagnetic properties of materials from the AAW structure: a) coaxial waveguide parts of the experimental setup; b) sample of the anti-radar coating of the Kh-101 missile; c) calculated electromagnetic characteristics of the material from the Kh-101 missile; d) material of the Shahed-136 (Geran-2) UAV body; e) measured values of the reflection coefficient compared to copper

Software experiment to determine radar visibility characteristics. Radar visibility characteristics were evaluated Shooting and Bounced Ray method (SBR+) by conducting a software experiment using a software and hardware complex for modelling high-frequency aspects of the functioning of weapons and military equipment samples based on Ansys Academic Research HF ver. 2025 R2. The experiment methodology consisted of creating an HFSS project, importing a prepared solid model (consisting of separate parts), assigning materials with appropriate electromagnetic properties to the parts, and determining the frequencies and irradiation angles under study. The frequencies were selected in accordance with the operating ranges of existing radar detection systems for airborne objects: F = 0.2÷15 GHz. All angles (4π steradian) were studied for further analysis of both ground-based and airborne (aircraft, aerostat) radar systems.

Statistical estimates of radar visibility characteristics were made by determining the median RCS values for different angles of monostatic radar observation (Fig. 6).

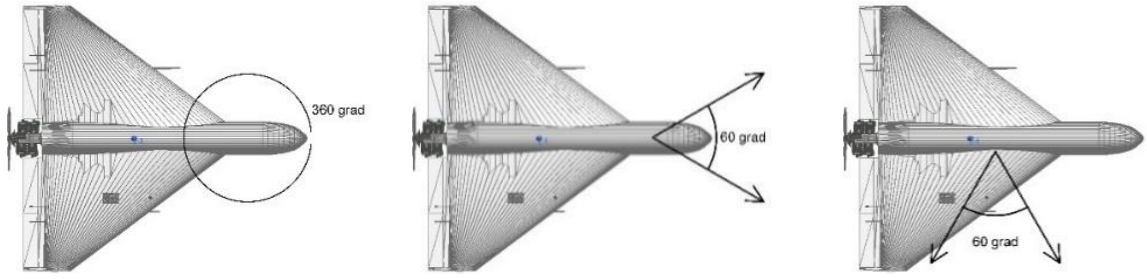

a) b) c)

Figure 6. Example of the angles studied to determine the median RCS values in the azimuth (course) plane: a) ring (circular); b) frontal; c) side

Results of determining radar visibility characteristics. Based on the results of software experiments, the primary data for further analysis were determined by the reverse secondary radiation diagrams (RCS dependence on the observation angle) (Fig. 7).

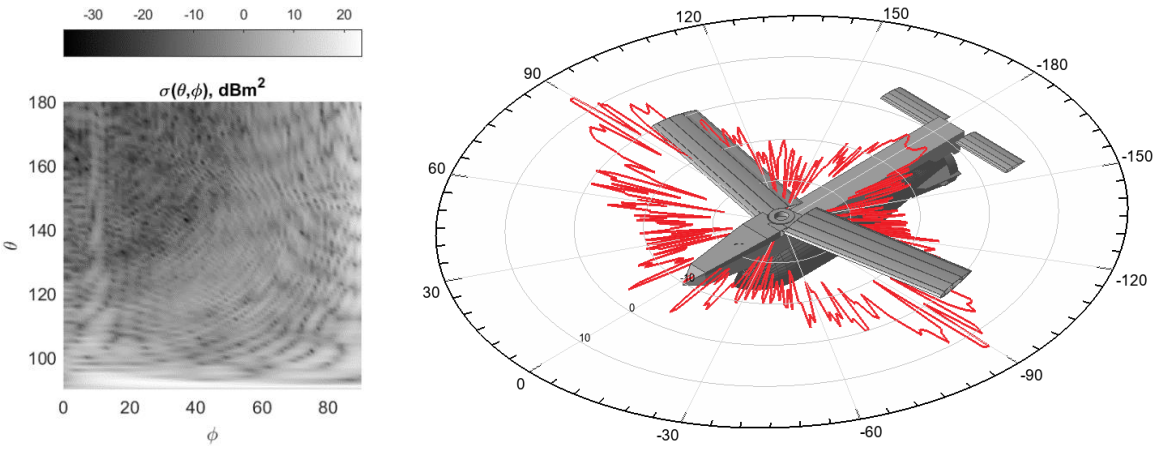

a) b)

Figure 7. Example of software experiment results: a) reverse secondary radiation pattern for the lower hemisphere of the UMPC with FAB-250 (F = 3 GHz); b) results of RCS calculation in the azimuth (course) plane (zero angle corresponds to the course orientation direction)

The results of software experiments to determine the reverse secondary radiation pattern of the AAW in the azimuth (course) plane are shown in Fig. 8.

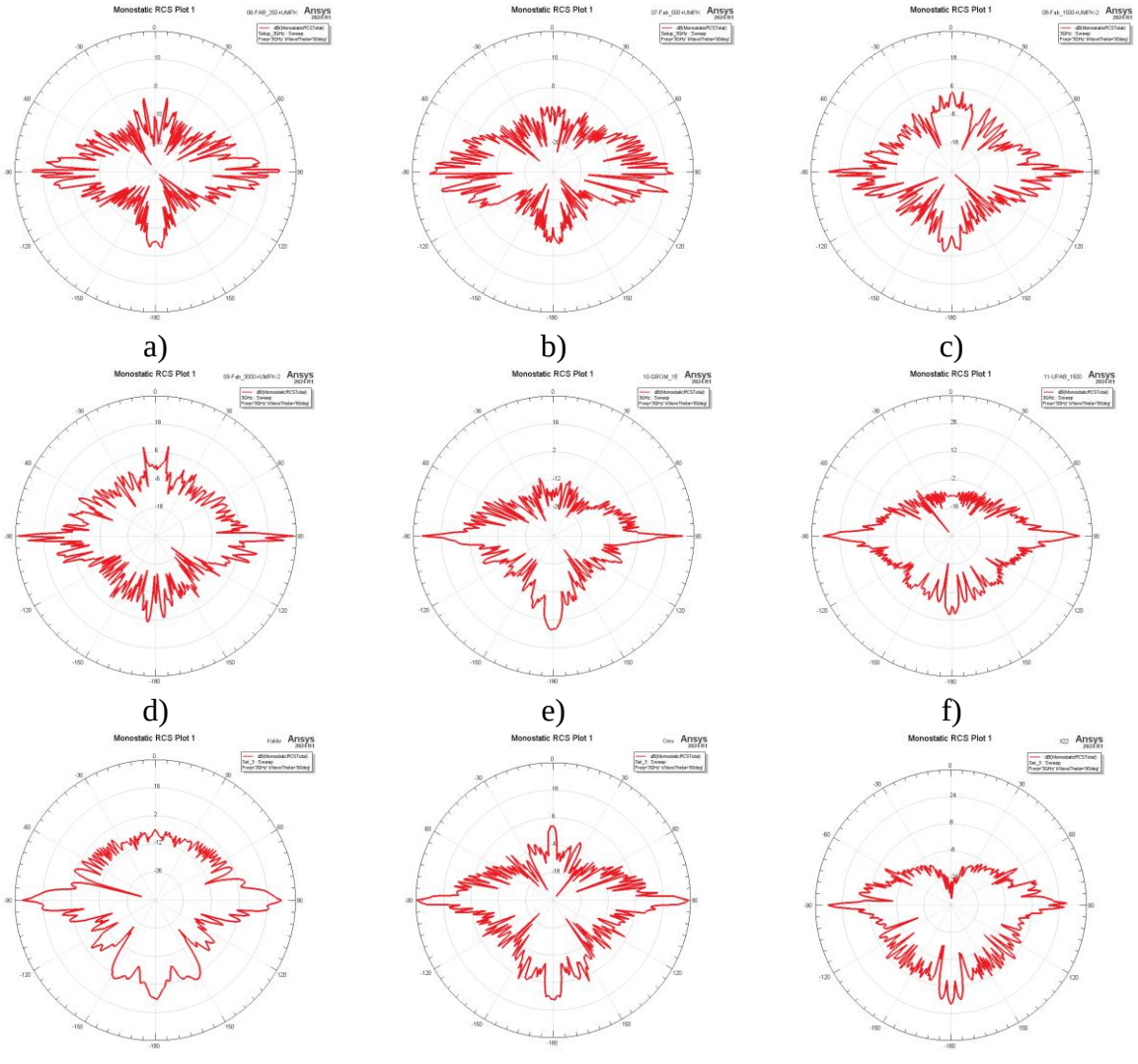

a) b) c)

d) e) f)

g) i) k)

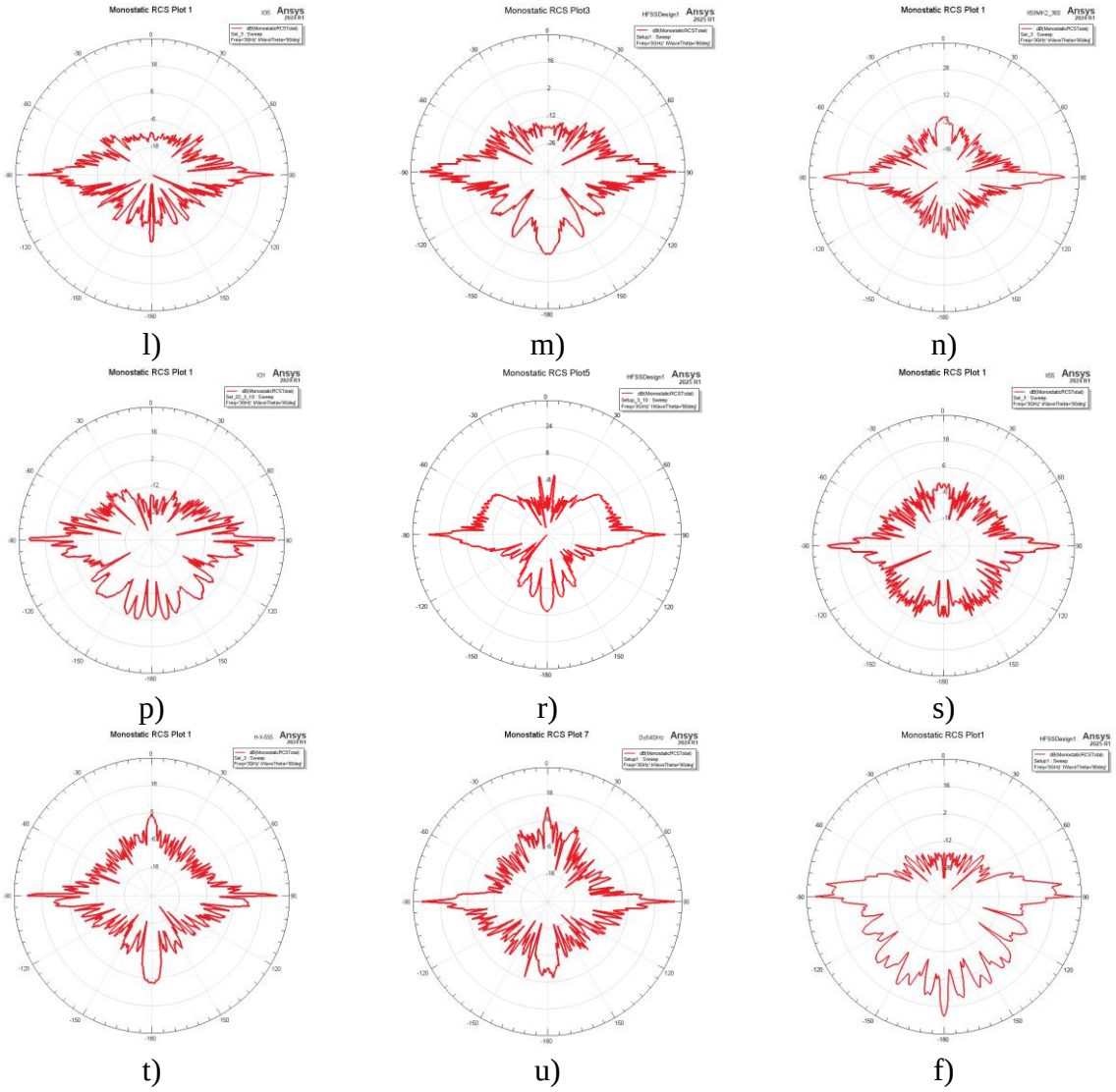

Figure 8. Reverse secondary radiation diagrams in the azimuth (course) plane for a frequency of 3 GHz (numbering corresponds to AAW from Fig. 1)

It should be noted that in real cases at real detection ranges of airborne objects (tens to hundreds of kilometers), the predominant observation angles relative to the azimuth (course) plane do not exceed 0.5-1 degree. (except for ballistic and aeroballistic missiles), i.e., the data shown in Fig. 8 is sufficient to evaluate the radar visibility characteristics for most practical cases.

Analysis of the reverse secondary radiation diagrams shows that AAW differ in terms of RCS levels. Differences are observed both in terms of the overall average (median) value and for different observation angles. Information about the statistical characteristics of the RCS of UAVs for given observation angles can be used as an additional feature for identifying the class of an air object. At the same time, existing models of radar detection and tracking of airborne objects make limited use of information about the RCS of the target and do not take into account information about the observation angle.

The results of software experiments are subject to further statistical processing (Fig. 9) for each group of angles.

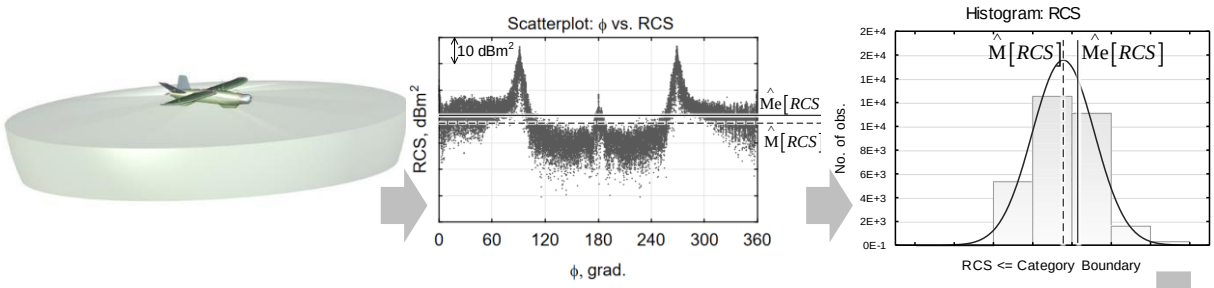

a) b) c)

RCS Characteristic	Value
Mean	$\hat{M}[RCS]$
Standard Deviation	5.58 dBm²
Maximum values	$\hat{M}[RCS]$+ (20…30) dBm²
Angles of maximum radar visibility	90 degrees and 270 degrees
Minimum values	$\hat{M}[RCS]$– (5…20) dBm²
Angle of minimum radar visibility	110-250 degrees (except 175-185 degrees)
Belonging to standard distribution laws	not confirmed

d)

Figure 9. Stages of statistical processing of information: a) example of the area of studied angles; b) example of a scatter plot; c) example of a distribution histogram and a hypothetical distribution law; d) example of individual statistical characteristics

Airborne objects used by the enemy to create a false air situation and overload air defense systems are equipped with Luneburg lens-type radar reflectors (Fig. 10). The methodology for studying reflectors consisted of studying the properties of materials, creating software models, and conducting software experiments [24]. The characteristics obtained were compared with optimal samples and also verified by conducting physical experiments.

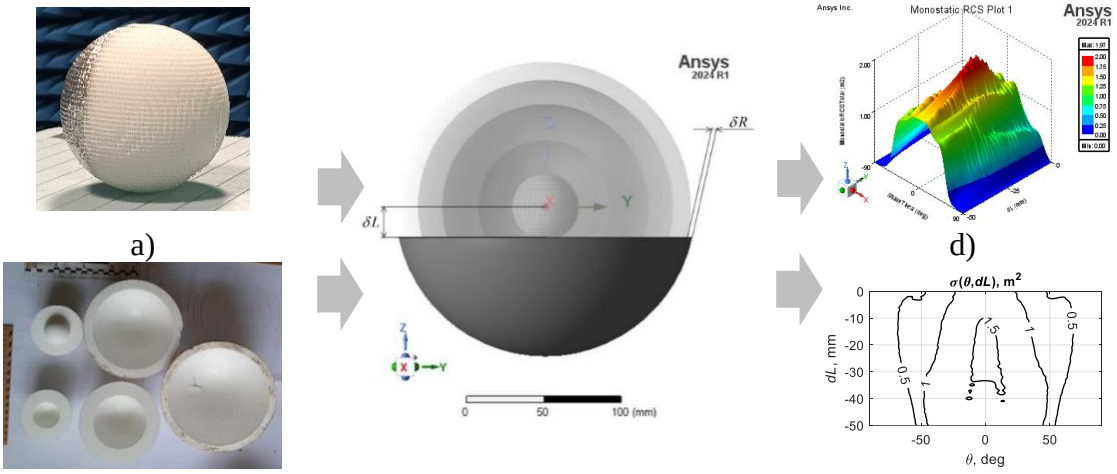

a) b) c) d) e)

Figure 10. Example of research on Luneburg lens reflectors: a) from the Parody UAV; b) from the E95M UAV; c) 3D software model; d) example of parametric analysis results; e) example of post-processing of results

The enemy also takes measures to equip individual air defense systems with both active and passive dipole jamming devices in the form of L-504 anti-radar missile launchers. The anti-radar projectile consists of 2-3 types of dipoles that form interference in the operating ranges of the radar equipment of anti-aircraft missile systems (Fig. 11).

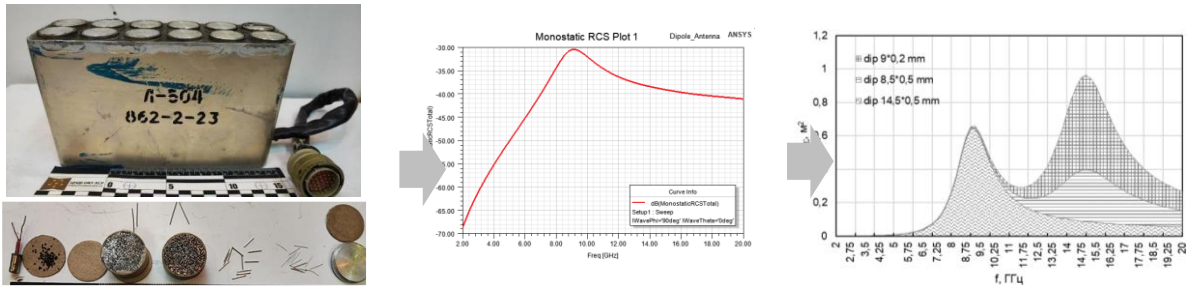

a) b) c)

Figure 11. Example of a study of dipole interference from the L-504 block of the Kh-101 missile: a) external view of the L-504 block and the equipment of one of the anti-radar projectiles; b) example of a study of the frequency dependence of the radar characteristics of one type of dipole; c) averaged estimates of the RCS of a cloud of dipoles created by one type of projectile

Discussion

Practical work has confirmed that the methodological basis for research into the characteristics of radar visibility of air attack means is appropriate to use: formalization of the characteristics of the shape, size and materials of real objects; creation of 3D models; model experiments to calculate the indicators of reflective properties when irradiated from different angles.

Research into the differences in the radar characteristics of real air targets compared to simulators and passive interference allows us to substantiate the directions for increasing the efficiency of detection and tracking of air attack means.

A further direction for research into the characteristics of radar visibility can be determined as the development of methods for using additional signal (energy) features to identify air objects and assessing the influence of trajectory characteristics on the angle of irradiation and conditions of radar detection.

Conclusions

A scientific and methodological approach to studying the characteristics of radar visibility of

modern air attack means has been developed and tested, which is based on the integration of the results of technical expertise of the remains of equipment, parametric 3D modeling and numerical methods for solving electrodynamic equations (SBR+ method).

A library of verified high-precision 3D models of the main samples of guided and unguided weapons of the Russian Federation (series of missiles Kh-101, Kh-59, 3M-14 "Caliber", aerial bombs with UMPK modules, Shahed-136/131 type UAVs) has been created, which take into account their internal layout, the presence of radio-transparent and radio-absorbing elements.

The electromagnetic properties of structural materials and coatings of captured samples of ZPN have been experimentally determined. The use of refined values of dielectric and magnetic permeability in the Ansys HFSS environment allowed to increase the reliability of the results of modeling the effective scattering surface (ESS) in a wide frequency range (0.2–15 GHz).

Quantitative indicators and angular dependences of the ESS for the studied objects in the 4π-steridian space were obtained. The results confirm a significant fluctuation of the radar visibility values depending on the irradiation angle, which allows to determine the most “vulnerable” sectors for target detection by ground and airborne radars.

A comparative analysis of the signatures of real air attack means and means of simulating the air situation (Lüneberg lenses, dipole reflectors) was carried out. The differences identified in the statistical characteristics of the returned secondary radiation create the basis for improving target selection algorithms and countering enemy electronic warfare means.

The practical significance of the work lies in the possibility of using the obtained data to configure air defense systems, develop new signatures for libraries of automated fire control systems, and optimize the placement of radar posts taking into account the terrain and predicted flight routes of the anti-aircraft missile system.

Список використаних джерел

[1.] Y. E. Riapolov, V. A. Vasylets, and O. Y. Sukharevskyi, "Dispersion characteristics of RQ-4B Global Hawk unmanned aerial vehicle in the centimetre and decimetre wavelength ranges," Science and Technology of the Air Force of the Armed Forces of Ukraine, vol. 16, no. 3, pp. 25–28, 2014.

[2.] T. Watanabe and H. Yamada, "Far-field radar cross section determination from near-field 3-D synthetic aperture imaging with arbitrary antenna-scanning surfaces," IEEE Transactions on Antennas and Propagation, vol. 70, no. 7, pp. 5831–5840, 2022, *https://doi.org/10.1109/TAP.2022.3161491*.

[3.] V. Semkin et al., "Analysing radar cross section signatures of diverse drone models at mm wave frequencies," IEEE Access, vol. 8, pp. 48958–48969, 2020, *https://doi.org/10.1109/ACCESS.2020.2979339*.

[4.] J. W. Crispin and A. L. Maffett, "Radar cross-section estimation for simple shapes," Proceedings of the IEEE, vol. 53, no. 8, pp. 833–848, 1965, *https://doi.org/10.1109/PROC.1965.4062*.

[5.] O. I. Sukharevskyi, V. O. Vasylets, S. V. Nechytailo, et al., Scattering of Electromagnetic Waves by Air and Ground Objects, O. I. Sukharevskyi, Ed. Kharkiv, Ukraine: KNAFU, 2009. (in Ukrainian)

[6.] A. L. Maffett, Topics for a Statistical Description of Radar Cross Section, 2nd ed. New York, NY, USA: Wiley-Interscience, 1989.
[7.] C. J. Li and H. Ling, "Radar signatures of small consumer drones," in Proc. IEEE Int. Symp. Antennas Propag. (AP-S/USNC-URSI), Fajardo, Puerto Rico, 2016.
[8.] Á. D. De Quevedo, F. I. Urzaiz, J. G. Menoyo, and A. A. López, "Drone detection and RCS measurements with ubiquitous radar," in Proc. Int. Conf. Radar (RADAR), Brisbane, QLD, Australia, 2018, pp. 1–6, *https://doi.org/10.1109/RADAR.2018.8557320*.
[9.] J. Farlik et al., "Radar cross section and detection of small unmanned aerial vehicles," in Proc. 17th Int. Conf. Mechatronics - Mechatronika (ME), 2016, pp. 1–7.
[10.] A. Schroder et al., "Numerical and experimental radar cross section analysis of the quadrocopter DJI Phantom 2," in Proc. IEEE Radar Conf., 2015, pp. 463–468.
[11.] C. J. Li and H. Ling, "An investigation on the radar signatures of small consumer drones," IEEE Antennas Wirel. Propag. Lett., vol. 16, pp. 649–652, 2017.
[12.] P. Sedivy and O. Nemec, "Drone RCS statistical behaviour," in NATO Modelling & Simulation Group, Sensors & Electronics Technology Panel, Science and Technology Organization, Specialists' meeting on drone detectability: Modelling the relevant signature (MSG_SET-183 RSM).
[13.] I. Bouzayene, K. Mabrouk, A. Gharsallah, and D. Kholodnyak, "Scan radar using an uniform rectangular array for drone detection with low RCS," in Proc. 19th Mediterranean Microwave Symp. (MMS), Hammamet, Tunisia, 2019, pp. 1–4, *https://doi.org/10.1109/MMS48040.2019.9157299*.
[14.] G. V. Pevtsov and M. M. Oleshchuk, "Analysis of the capabilities of RTV surveillance radars for detecting, tracking and identifying unmanned aerial vehicles," Weapon Systems and Military Equipment, no. 3(67), pp. 24–30, 2021, *https://doi.org/10.30748/soivt.2021.67.03*.
[15.] M. Pieraccini, L. Miccinesi, and N. Rojhani, "RCS measurements and ISAR images of small UAVs," IEEE Aerospace and Electronic Systems Magazine, vol. 32, pp. 28–32, 2017, *https://doi.org/10.1109/MAES.2017.160167*.
[16.] V. P. Ryabukha, "Radar surveillance of unmanned aerial vehicles (overview)," Radioelectronics and Communications Systems, vol. 63, no. 11, pp. 1–22, 2020, *https://doi.org/10.20535/S0021347020110011*.
[17.] I. D. Olin and F. D. Queen, "Dynamic measurement of radar cross sections," Proceedings of the IEEE, vol. 53, no. 8, pp. 954–961, 1965, *https://doi.org/10.1109/PROC.1965.4074*.
[18.] M. Ezuma, M. Funderburk, and I. Guvenc, "Compact-range RCS measurements and modeling of small drones at 15 GHz and 25 GHz," in Proc. IEEE Radio and Wireless Symp. (RWS), 2020, pp. 313–316, *https://doi.org/10.1109/RWS45077.2020.9050049*.
[19.] O. Sukharevsky, V. Vasilets, S. Nechytailo, A. Reznichenko, and H. Kudriashov, "Radar characteristics study of the model of 'Shahed-136' barraging munition," Science and Technology of the Air Force of the Armed Forces of Ukraine, no. 2(51), pp. 56–62, 2023, *https://doi.org/10.30748/nitps.2023.51.07*.
[20.] O. Borysenko, "Characteristics of secondary radiation of cruise missiles 3M-14 Calibr and Kh-101 in the VHF band," Science and Technology of the Air Force of the Armed Forces of Ukraine, no. 1(54), pp. 68–76, 2024, *https://doi.org/10.30748/nitps.2024.54*.
[21.] J. Baker-Jarvis, M. D. Janezic, J. H. Grosvenor, Jr., and R. G. Geyer, "Transmission/reflection and short-circuit line methods for measuring permittivity and permeability," National Institute of Standards and Technology (NIST), Tech. Note 1355-R, 1993.
[22.] W. B. Weir, "Automatic measurement of complex dielectric constant and permeability at microwave frequencies," Proceedings of the IEEE, vol. 62, no. 1, pp. 33–36, 1974, *https://doi.org/10.1109/PROC.1974.9382*.
[23.] D. M. Pozar, Microwave Engineering, 4th ed. Hoboken, NJ, USA: John Wiley & Sons, Inc., 2012.
[24.] D. S. Zavadskyi, "Results of research on the radar reflector of the Luneberg lens type," Scientific and Technical Journal: State Research Institute for Testing and Certification of Armaments and Military Equipment, no. 2(8), pp. 75–81.

Завадський Дмитро Станіславович
https://orcid.org/0000-0003-2728-136X
Білобородов Олег Олександрович **(доктор технічних наук, старший дослідник)**
https://orcid.org/0000-0003-3166-2659

Центральний науково-дослідний інститут озброєння та військової техніки Збройних Сил України, Київ, Україна

ДОСЛІДЖЕННЯ ХАРАКТЕРИСТИК РАДІОЛОКАЦІЙНОЇ ПОМІТНОСТІ ЗАСОБІВ ПОВІТРЯНОГО НАПАДУ рф ІЗ ЗАСТОСУВАННЯМ ТЕХНОЛОГІЙ 3D-МОДЕЛЮВАННЯ

У статті представлено науково-методичні підходи та результати досліджень характеристик радіолокаційної помітності сучасних засобів повітряного нападу противника з використанням числових методів моделювання. Для проведення програмного експерименту застосовується програмно-технічний комплекс моделювання високочастотних аспектів функціонування зразків озброєння та військової техніки на

базі Ansys Academic Research HF у поєднанні з параметричним 3D-моделюванням у SolidWorks та аналогічних САПР. Проведено створення та дослідження 3D-моделей основних засобів повітряного нападу РФ, зокрема крилатих і аеробалістичних ракет (Х-22, Х-55, Х-59, Х-69, Х-101 тощо), а також авіаційних бомб із планеруючими модулями (УМПК з ФАБ-250, ФАБ-500, ФАБ-1500 тощо). Особливу увагу приділено визначенню електромагнітних властивостей матеріалів, що використовуються у конструкціях зразків, за методикою NIST із подальшим введенням отриманих параметрів у середовище моделювання. Проведено серію програмних експериментів у широкому діапазоні частот для оцінки ефективної площі розсіювання для різних ракурсів опромінення. Отримані результати дозволили визначити статистичні характеристики радіолокаційної помітності різних типів повітряних цілей, виявити вплив геометрії та матеріалів на значення ефективної площі розсіювання і забезпечити основу для подальших досліджень у сфері радіолокаційного виявлення та супроводження повітряних об'єктів.

Ключові слова: *радіолокаційна помітність, ефективна площа розсіювання, засоби повітряного нападу, 3D-моделювання, Ansys HFSS, електромагнітні властивості матеріалів.*

Список використаних джерел

[1.] Y. E. Riapolov, V. A. Vasylets, and O. Y. Sukharevskyi, "Dispersion characteristics of RQ-4B Global Hawk unmanned aerial vehicle in the centimetre and decimetre wavelength ranges," Science and Technology of the Air Force of the Armed Forces of Ukraine, vol. 16, no. 3, pp. 25–28, 2014.

[2.] T. Watanabe and H. Yamada, "Far-field radar cross section determination from near-field 3-D synthetic aperture imaging with arbitrary antenna-scanning surfaces," IEEE Transactions on Antennas and Propagation, vol. 70, no. 7, pp. 5831–5840, 2022, *https://doi.org/10.1109/TAP.2022.3161491*.

[3.] V. Semkin et al., "Analysing radar cross section signatures of diverse drone models at mm wave frequencies," IEEE Access, vol. 8, pp. 48958–48969, 2020, *https://doi.org/10.1109/ACCESS.2020.2979339*.

[4.] J. W. Crispin and A. L. Maffett, "Radar cross-section estimation for simple shapes," Proceedings of the IEEE, vol. 53, no. 8, pp. 833–848, 1965, *https://doi.org/10.1109/PROC.1965.4062*.

[5.] О. І. Сухаревський, В. О. Василець, С. В. Нечитайло та ін., Розсіювання електромагнітних хвиль повітряними та наземними об'єктами, О. І. Сухаревський, Ред. Харків, Україна: ХНУПС, 2009.

[6.] A. L. Maffett, Topics for a Statistical Description of Radar Cross Section, 2nd ed. New York, NY, USA: Wiley-Interscience, 1989.

[7.] C. J. Li and H. Ling, "Radar signatures of small consumer drones," in Proc. IEEE Int. Symp. Antennas Propag. (AP-S/USNC-URSI), Fajardo, Puerto Rico, 2016.

[8.] Á. D. De Quevedo, F. I. Urzaiz, J. G. Menoyo, and A. A. López, "Drone detection and RCS measurements with ubiquitous radar," in Proc. Int. Conf. Radar (RADAR), Brisbane, QLD, Australia, 2018, pp. 1–6, *https://doi.org/10.1109/RADAR.2018.8557320*.

[9.] J. Farlik et al., "Radar cross section and detection of small unmanned aerial vehicles," in Proc. 17th Int. Conf. Mechatronics - Mechatronika (ME), 2016, pp. 1–7.

[10.] A. Schroder et al., "Numerical and experimental radar cross section analysis of the quadrocopter DJI Phantom 2," in Proc. IEEE Radar Conf., 2015, pp. 463–468.

[11.] C. J. Li and H. Ling, "An investigation on the radar signatures of small consumer drones," IEEE Antennas Wirel. Propag. Lett., vol. 16, pp. 649–652, 2017.

[12.] P. Sedivy and O. Nemec, "Drone RCS statistical behaviour," in NATO Modelling & Simulation Group, Sensors & Electronics Technology Panel, Science and Technology Organization, Specialists' meeting on drone detectability: Modelling the relevant signature (MSG_SET-183 RSM).

[13.] I. Bouzayene, K. Mabrouk, A. Gharsallah, and D. Kholodnyak, "Scan radar using an uniform rectangular array for drone detection with low RCS," in Proc. 19th Mediterranean Microwave Symp. (MMS), Hammamet, Tunisia, 2019, pp. 1–4, *https://doi.org/10.1109/MMS48040.2019.9157299*.

[14.] G. V. Pevtsov and M. M. Oleshchuk, "Analysis of the capabilities of RTV surveillance radars for detecting, tracking and identifying unmanned aerial vehicles," Weapon Systems and Military Equipment, no. 3(67), pp. 24–30, 2021, *https://doi.org/10.30748/soivt.2021.67.03*.

[15.] M. Pieraccini, L. Miccinesi, and N. Rojhani, "RCS measurements and ISAR images of small UAVs," IEEE Aerospace and Electronic Systems Magazine, vol. 32, pp. 28–32, 2017, *https://doi.org/10.1109/MAES.2017.160167*.

[16.] V. P. Ryabukha, "Radar surveillance of unmanned aerial vehicles (overview)," Radioelectronics and Communications Systems, vol. 63, no. 11, pp. 1–22, 2020, *https://doi.org/10.20535/S0021347020110011*.

[17.] I. D. Olin and F. D. Queen, "Dynamic measurement of radar cross sections," Proceedings of the IEEE, vol. 53, no. 8, pp. 954–961, 1965, *https://doi.org/10.1109/PROC.1965.4074*.

[18.] M. Ezuma, M. Funderburk, and I. Guvenc, "Compact-range RCS measurements and modeling of small drones at 15 GHz and 25 GHz," in Proc. IEEE Radio and Wireless Symp. (RWS), 2020, pp. 313–316, *https://doi.org/10.1109/RWS45077.2020.9050049*.

[19.] O. Sukharevsky, V. Vasilets, S. Nechytailo, A. Reznichenko, and H. Kudriashov, "Radar characteristics study of the model of 'Shahed-136' barraging munition," Science and Technology of the Air Force of the Armed Forces of Ukraine, no. 2(51), pp. 56–62, 2023, *https://doi.org/10.30748/nitps.2023.51.07*.

[20.] O. Borysenko, "Characteristics of secondary radiation of cruise missiles 3M-14 Calibr and Kh-101 in the VHF band," Science and Technology of the Air Force of the Armed Forces of Ukraine, no. 1(54), pp. 68–76, 2024, *https://doi.org/10.30748/nitps.2024.54*.

[21.] J. Baker-Jarvis, M. D. Janezic, J. H. Grosvenor, Jr., and R. G. Geyer, "Transmission/reflection and short-circuit line methods for measuring permittivity and permeability," National Institute of Standards and Technology (NIST), Tech. Note 1355-R, 1993.

[22.] W. B. Weir, "Automatic measurement of complex dielectric constant and permeability at microwave frequencies," Proceedings of the IEEE, vol. 62, no. 1, pp. 33–36, 1974, *https://doi.org/10.1109/PROC.1974.9382*.

[23.] Pozar, Microwave Engineering, 4th ed. Hoboken, NJ, USA: John Wiley & Sons, Inc., 2012.

[24.] D. S. Zavadskyi, "Results of research on the radar reflector of the Luneberg lens type," Scientific and Technical Journal: State Research Institute for Testing and Certification of Armaments and Military Equipment, no. 2(8), pp. 75–81.